



# The curvature peaks of the trajectory of the body centre of mass during walking: A new index of dynamic balance

Chiara Malloggi<sup>a</sup>, Stefano Scarano<sup>a,b</sup>, Valeria Cerina<sup>a</sup>, Luigi Catino<sup>b</sup>, Viviana Rota<sup>a</sup>, Luigi Tesio<sup>a,b,\*</sup>

<sup>a</sup> Istituto Auxologico Italiano, IRCCS, Department of Neurorehabilitation Sciences, Ospedale San Luca, Milano, Italy

<sup>b</sup> Department of Biomedical Sciences for Health, Università degli Studi di Milano, Milano, Italy

## ARTICLE INFO

### Article history:

Accepted 21 April 2021

### Keywords:

Centre of mass  
Curvature  
Walking  
Balance  
Rehabilitation

## ABSTRACT

During walking, falling is most likely to occur towards the side of the supporting lower limb during the single stance. Timely lateral redirection of the centre of mass (CoM) preceding the no-return position is necessary for balance. We analysed the curvature peaks (the inverse of the radius of curvature) of the three-dimensional path of the CoM during the entire stride. Twelve healthy adults walked on a force-sensorized treadmill at constant velocities from 0.4 to 1.2 m s<sup>-1</sup>, in 0.2 m s<sup>-1</sup> increments. The three-dimensional displacements of the CoM, the muscular power sustaining the CoM motion with respect to the ground, and the efficiency of the pendulum-like transfer of the CoM were computed via the double integration of the ground reaction forces. The curvatures of the CoM trajectory were measured (Frenet-Serret formula). During the single stance, the curvature showed a bell-shaped increment, lasting a few tenths of a millisecond, and peaking at 365–683 m<sup>-1</sup> (radius of 2.7–1.4 mm, respectively), the higher the walking velocity. The CoM was redirected towards the swinging lower limb. The curvature increment was sustained by muscle-driven braking of the CoM. Smoother increments of curvature (peaking at approximately 37–150 m<sup>-1</sup>), further orienting the CoM towards the leading lower limb, were observed during the double stance. The peaks of the curvatures were symmetric between the two sides. The high curvature peaks during the single stance may represent an index of dynamic balance during walking. This index might be useful for both rehabilitation and sports training purposes.

© 2021 The Authors. Published by Elsevier Ltd. This is an open access article under the CC BY-NC-ND license (<http://creativecommons.org/licenses/by-nc-nd/4.0/>).

## 1. Introduction

Maintaining balance during walking is challenging. A fall is most likely to occur sideways during the single stance (Smeesters et al., 2001). A recent review examined different methods for quantifying dynamic balance, and no consensus has been reached concerning the most suitable measure (Siragy and Nantel, 2018). A laboratory-based measure for evaluating balance performance during walking has been developed: the margin of stability (MOS) (Hof et al., 2005). The MOS is the distance between the horizontal position of the centre of mass (CoM) times a factor reflecting the CoM velocity (extrapolated centre of mass, xCoM) and the perimeter of the individual's base of support at any given instant (Hof, 2008, 2007; Hof et al., 2007). This has been widely used for the assessment of balance during walking undergoing various perturbations (Gates et al., 2013; Hof et al., 2007; Hurt et al.,

2011; Mc Andrew Young et al., 2012; Okubo et al., 2018; Rogers et al., 2001), at various ages (Bierbaum et al., 2010; Hurt and Grabiner, 2015), and in patients suffering from various motor impairments (Hak et al., 2013; Kao et al., 2014; Vistamehr et al., 2016).

Lateral placement of the swinging foot – step width – creates the initial condition to control lateral CoM motion because of the narrow width of the base of support during the single stance phase (Bauby and Kuo, 2000; Hurt et al., 2011; MacKinnon and Winter, 1993; Rosenblatt and Grabiner, 2010). However, little is known about the neuromotor mechanisms that ensure stability during the single stance. Straight walking *per se*, ideally, should not require lateral displacement of the CoM; however, it is necessary to alternate loading on the two opposite lower limbs, thus perpetuating the pendulum-like motion of every single limb in the sagittal plane. Therefore, lateral redirection of the CoM is unavoidable (Cavagna et al., 2002). The ensuing lateral motion can be considered an inverted pendulum in the frontal plane. The lateral redirection of the CoM must occur before reaching the no-return point, beyond which an irreversible sideways fall begins unless a sideways step is performed. Pivoting on a single leg could be passive,

\* Corresponding author at: Istituto Auxologico Italiano, IRCCS, Department of Neurorehabilitation Sciences, Ospedale San Luca, via Giuseppe Mercalli 32, 20122 Milan, Italy.

E-mail addresses: [luigi.tesio@unimi.it](mailto:luigi.tesio@unimi.it), [l.tesio@auxologico.it](mailto:l.tesio@auxologico.it) (L. Tesio).

but the spontaneous period of oscillation of the CoM is incompatible with most of the velocity/cadence combinations adopted during walking (Hof, 2008). Therefore, before the point of no-return is reached on the supporting leg, active corrections of the CoM trajectory are needed. In this study, only straight-line level walking at constant average speeds in healthy adults was considered. We hypothesize that the curvature peak (the inverse of the radius) of the three-dimensional (3D) path of the CoM during the single stance phase may represent an index of the motor skill underlying the timely and effective control of lateral CoM redirection. This parameter was analysed during walking at different velocities.

## 2. Materials and methods

### 2.1. Participants

Twelve healthy volunteers were enrolled. Inclusion criteria were the ability to understand instructions, sign the informed consent form, and complete the locomotion task; age 18–60 years; the absence of neurologic or orthopaedic conditions affecting gait. Exclusion criteria were surgical orthopaedic interventions on the lower limbs or spine in the previous 18 months; symptomatic joint or spine diseases; experience of walking on treadmills during the previous six months.

### 2.2. Ethics

The experiments were conducted according to the Declaration of Helsinki of the World Medical Association (2013) and approved by the local ethics committee. All participants provided written informed consent before participation.

### 2.3. Equipment

Participants were asked to walk on a split-belt force-sensorized treadmill (ADAL 3D; Médical Développement, Andrézieux-Bouthéon, France) mounted on eight 3D piezoelectric force sensors (KI 9048B; Kistler, Winterthur, Switzerland). Force signals were sampled at 250 Hz. The two half-treadmills ran at the same speed, and force signals from both sides were vectorially summed, thus reproducing the signals generated from a single-belt treadmill (Tesio et al., 2010).

### 2.4. Experimental protocol

Participants wore a t-shirt, shorts, and light gym shoes. Height and weight were recorded (scale accuracy: 2 mm and 50 g, respectively). Participants were allowed to adapt to walking on the treadmill for approximately 30 s at each velocity. During walking, participants were asked to look at a black spot (8 cm diameter) placed approximately 2 m in front of the treadmill at eye level on a white wall.

During the trial, participants were asked to walk for at least 45 s at increasing velocities from 0.4 to 1.2 m s<sup>-1</sup>, in 0.2 m s<sup>-1</sup> increments. Participants were warned before each speed change, which took 5 s in a ramp-like fashion. The experimental conditions provided high reproducibility of results, thanks to the known and constant speed imposed by the treadmill (Tesio and Rota, 2008).

### 2.5. Analysis

Force signals were synchronised and analysed offline with algorithms available within the SMART Software Suite (BTS Bioengineering Spa, Milan, Italy). For each speed, data were averaged across six subsequent strides for each participant. The stride period

(one stride equals two consecutive steps) was defined as the interval between two subsequent toe-offs of the posterior foot, normalised to 100 time points. Toe-off was defined as the instant the vertical force under the foot decreased below 30 N (Tesio and Rota, 2008). The step period was defined as the interval between the toe-off of the opposite foot and the subsequent toe-off of the corresponding foot. The side of the double stance was defined as the side of the posterior foot. In gait studies, it is customary to initiate a step at foot strike. The present unusual criterion (toe-off) for defining the stride and step periods focused attention on the single stance phases, when the extreme lateral displacement of the CoM occurs, thus highlighting the perspective of dynamic balance. Videos of the trials were inspected offline to ascertain the absence of rough irregularities (e.g., stumbling).

#### 2.5.1. The trajectory of the CoM path

The displacements of the CoM in the 3D space were obtained via double integration of the ground reaction forces. These were analysed using the double integration or “Newtonian” method: accelerations, velocity changes and 3D displacements were computed from force records (Cavagna, 1975; Cavagna et al., 1983). If the displacement caused by the mean forward velocity is subtracted from the velocity changes, the CoM path during the stride can be represented as a cyclic and virtually closed (on an average of strides) 3D displacement around an average position. The path takes a figure-of-eight shape (dubbed the “bow-tie”), about 16 cm long, upwardly concave in the frontal plane (Malloggi et al., 2019b; Tesio et al., 2011, 2010).

#### 2.5.2. Energy transfer and power in the CoM motion

Walking has been traditionally modelled as an inverted pendulum (Alexander, 2005) with its CoM undergoing periodic changes in forward, lateral, and vertical kinetic energies ( $E_{kf}$ ,  $E_{kl}$ , and  $E_{kv}$ , respectively) and gravitational potential energy ( $E_p$ ). The energy due to the vertical motion of the CoM is computed as  $E_v = E_{kv} + E_p$ . The sum of  $E_{kf}$ ,  $E_{kl}$ , and  $E_v$  gives the total mechanical energy of the CoM,  $E_{tot}$ . An ideal pendulum allows for a fully passive exchange between  $E_{kf}$ ,  $E_{kl}$ , and  $E_v$ , to ensure that  $E_{tot}$  remains constant. However, no real pendulum is fully conservative; changes in  $E_{tot}$  occur. These changes (neglecting air and body frictional forces) can only be sustained by muscle work called “external work”,  $W_{ext}$ ; this is necessary to keep the body CoM in motion with respect to the ground. At each instant, the changes in  $E_{tot}$  give the corresponding work values:  $W_f$  for  $E_{kf}$ ,  $W_v$  for  $E_v$ ,  $W_l$  for  $E_{kl}$ , and  $W_{ext}$  for  $E_{tot}$ , respectively (Rota et al., 2016; Tesio et al., 2011). Power was computed here as the first derivative of work. Conventionally, work and power subtending increments or decrements of  $E_{tot}$  are defined as positive or negative, respectively (Cavagna et al., 1976). The instantaneous efficiency of the kinetic-potential energy transfer of the CoM was computed as the instantaneous recovery index,  $R$  (0% = no recovery, 100% = complete recovery, i.e., fully passive CoM translation), using the formula (Cavagna, 1975; Cavagna et al., 2002; Tesio et al., 1998):

$$R = \frac{|W_f| + |W_l| + |W_v| - |W_{ext}|}{|W_f| + |W_l| + |W_v|} \times 100 \quad (1)$$

$R$  can result from different combinations of “positive” and “negative” work values. For instance, during the “fall” phase of the single stance, when the CoM is directed downward, forward and laterally, any “braking” action of the muscles, causing deceleration, may turn into negative work values, including a negative  $W_{ext}$ :  $R$  will remain positive, below 100%. A zero  $R$  indicates that no exchange occurs between  $E_v$  and  $E_{kf}$  or  $E_{kl}$ , regardless of whether the observed changes represent increments or decrements of mechanical energy.

### 2.5.3. The curvature of the CoM path

The path curvature (inverse of the radius of curvature) of the CoM during one stride was computed from the displacements of the CoM in the 3D space, according to the Frenet–Serret formulae (Tesio et al., 2011).

Given a particle moving along a continuous, differentiable curve in 3D Euclidean space, the Frenet–Serret formulae describes its kinematic properties:

$$\frac{d\mathbf{T}}{ds} = \kappa \mathbf{N} \quad (1)$$

$$\frac{d\mathbf{N}}{ds} = -\kappa \mathbf{T} + \tau \mathbf{B} \quad (2)$$

$$\frac{d\mathbf{B}}{ds} = -\tau \mathbf{N} \quad (3)$$

where  $\frac{d}{ds}$  is the derivative with respect to arclength;  $\kappa$  is the curvature;  $\tau$  is the torsion of the curve;  $\mathbf{T}$  is the unit vector tangent to the curve pointing in the direction of motion;  $\mathbf{N}$  is the normal unit vector: the derivative of  $\mathbf{T}$  with respect to the arclength parameter of the curve, divided by its length; and  $\mathbf{B}$  is the binormal unit vector, the cross product of  $\mathbf{T}$  and  $\mathbf{N}$ .

Maximum values of the path curvature in each walking phases (right single stance, ssR; right double stance, dsR; left single stance, ssL; left double stance, dsL) were computed and defined as curvature peaks.

The analysis was conducted with a custom-made MATLAB algorithm (version R2019b, MathWorks Inc., Natick, USA). Graphic representations were plotted using SigmaPlot™ (version 14.0, Systat Software Inc., San Jose, USA).

## 2.6. Statistics

The normality of the distribution of the variables was checked using the Shapiro–Wilk test. Continuous variables were expressed as means (standard deviation, SD), medians (the 5th–95th percentile range), while categorical data were expressed as absolute frequencies and percentages. The symmetry between the right and left curvature peaks was assessed by calculating the logarithm base 10 of the ratio between the peaks [to cope with the nonlinearity of proportions, (Cavagna et al., 1983; Tesio et al., 2010)], its SD value, and 95% tolerance and confidence limits. Variance is applied to estimated means with confidence limits; tolerance limits are applied to individual observations (Tesio et al., 2010) and are, therefore, wider (Altman and Bland, 1983; Cavagna et al., 1983). The effects of the walking velocities, the interaction across walking velocities and the phases on the curvature peaks (ssR, dsR, ssL, and dsL) were analysed, for each individual comparison, using a non-parametric analysis of variance model (Friedman ANOVA). The effect of the “participant” source of variance on the curvature peaks was also analysed using Friedman ANOVA. The effect of the phase (single vs double stance) was analysed using the Wilcoxon signed-rank test. In cases of significant Friedman ANOVA models (at  $P < 0.05$ ), Wilcoxon signed-rank post-hoc tests were run on contrasts between condition pairs. The Bonferroni correction ( $P$ -value set at 0.05 divided by the number of measures tested) was applied. The analysis was performed using StataSE™ (version 14.0; Stata Corp., College Station, USA).

## 3. Results

### 3.1. Participants

Table 1 gives the demographic and anthropometric participant information.

**Table 1**

Characteristics of study participants ( $n = 12$ ).

Gender (women; men)	6; 6		
	Mean (SD)	Median	5th–95th Percentile
Age, years	25.1 (3.0)	25.5	21.0–28.9
Height, m	1.72 (0.12)	1.73	1.56–1.89
Weight, kg	67.7 (12.3)	64.0	53.3–88.2
Body Mass Index, $\text{kg m}^{-2}$	22.7 (2.1)	22.4	20.2–25.8

SD, Standard deviation.

### 3.2. The curvature peaks of the CoM trajectory

Fig. 1 shows the morphologic and dynamic data of the 3D path of the CoM during one stride, from one representative participant (woman, 26 years, 1.55 m tall) walking at  $0.8 \text{ m s}^{-1}$ . Panel B zooms in on some of the tracings in panel A.

The stride began at toe-off of the right rear limb. Foot-ground contacts were marked by the bottom horizontal segments (“l” and “r” for the left and right foot, respectively). The curvature of the CoM trajectory (top tracing) presented with four peaks: ssR and ssL, for right and left steps, respectively, when they occurred around the middle of the single stance phases, and dsR and dsL, when they occurred during the double stance phases (right and left foot behind, respectively). The ssR and ssL were much higher than dsR and dsL. In both steps, all curvature peaks occurred when R (second tracing from the top) suddenly dropped from 100 to 0, indicating that the passive pendulum-like translation mechanism of CoM was briskly substituted by a muscle-driven mechanism, as previously noticed (Cavagna et al., 2002; Tesio et al., 2011).

At each step, the ssR and ssL peaks were roughly coincident with the minima of both  $E_{\text{kf}}$  and  $E_{\text{kl}}$  (3rd and 5th tracing from the top, respectively), maxima of  $E_v$  (4th tracing from the top) and with an approximately stable phase of  $E_{\text{tot}}$  of CoM (6th tracing from the top) of near-zero external-muscular power (7th tracing from the top). Fig. 1B zooms in on the second step and omits the kinetic and potential energy curves. It shows that the ssL peak initiated the braking of CoM’s forward (and lateral) motion. The ssL peak preceded the decrements of  $E_{\text{tot}}$  and the phase with negative external-muscular power values. Braking was muscle-driven (zero R values). In contrast, the dsL peak occurring at the beginning of the double stance corresponded to an acceleration phase of the CoM in the vertical, sagittal, and lateral directions, highlighted by the increments of  $E_{\text{tot}}$  and positive values of external power, P. This propulsion was fully muscle-driven (zero R values). In short, the higher peaks (ssR and ssL) underlie the lateral U-turns of the CoM, requiring the braking action of active muscles. Power was absorbed by CoM. This braking action (highlighted by the negative power values) acted in opposite directions: it initially prevented the CoM from trespassing the no-return point and then delayed the fall toward the unsupported side until the front foot strikes the ground (Fig. 1A, the coincidence of foot strike with the beginning of the push-off phase sustained by positive power). This implied that a succession of different muscles, all with a “braking” action on the CoM, was required. The lower peaks during the double stance (dsR and dsL) underlie the modest directional change towards the leading foot, occurring during push-off. In this step phase, most of the positive power required to keep the CoM in motion in the forward direction was provided (Tesio and Rota, 2019).

Fig. 2 frames the curvature peaks within space, neglecting the time variable, through polar graphs of the CoM displacements.

The differences in curvatures between the sharper ssR and ssL peaks and smoother dsR and dsL peaks can be appreciated more intuitively.

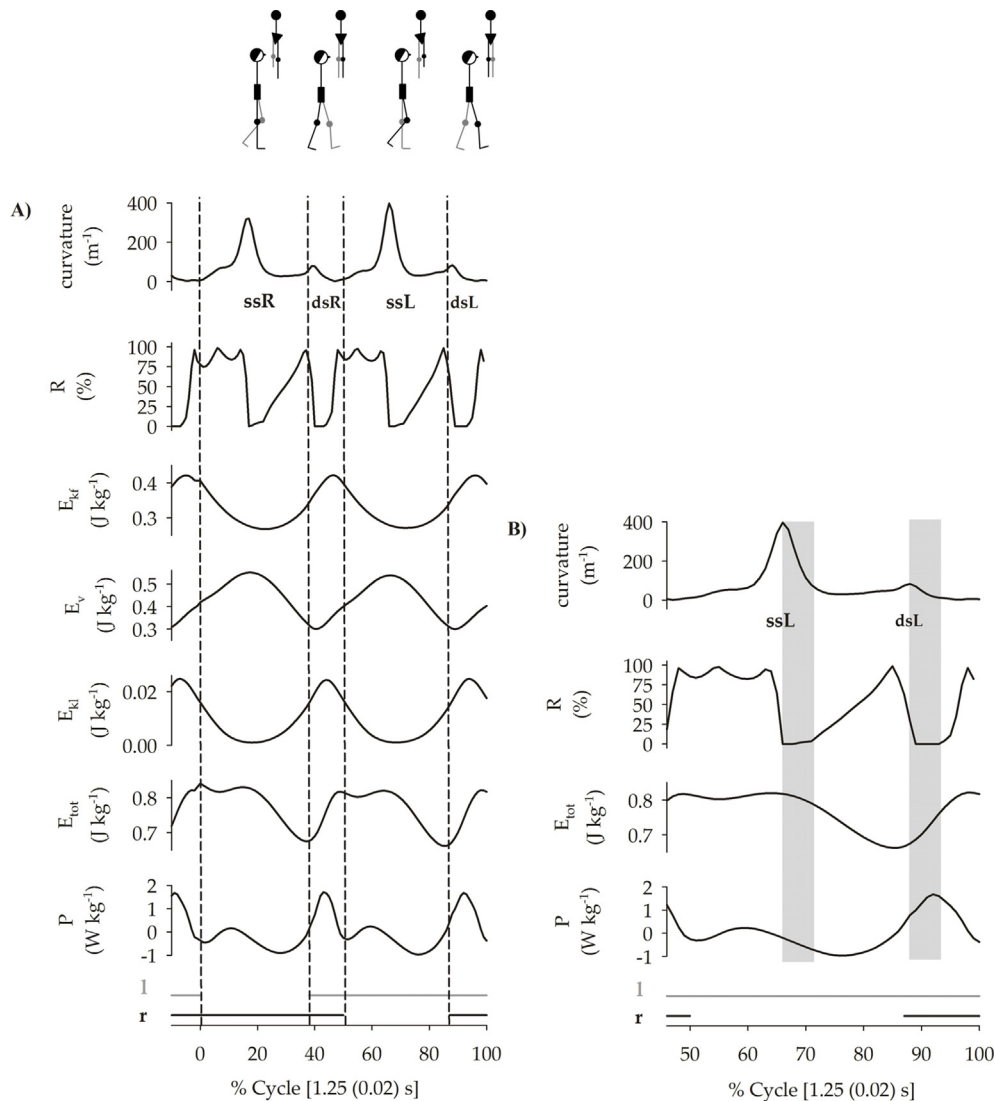


**Fig. 1.** The tracings refer to the average of 6 subsequent strides performed by a representative participant (woman, 26 years, 1.55 m tall) walking on a force-sensorised treadmill at  $0.8 m s^{-1}$ . In the left panel, the human outline forms on the top of the graph help visualise the mechanical phenomena along the path of the CoM during the stride. From top to bottom, the curves refer to the curvature of the CoM path; the instantaneous “percent recovery” of mechanical energy (R); the kinetic energy due to the forward velocity ( $E_{kf}$ ); the kinetic energy due to the vertical displacement plus the gravitational potential energy ( $E_v$ ); the kinetic energy due to the lateral velocity ( $E_{kl}$ ); the total mechanical energy ( $E_{tot}$ ), i.e., the sum of the above energies; and the external power (P) applied to the CoM, as a function of the normalised stride period (on the abscissa, absolute mean duration within brackets). The stride begins with the toe-off of the left (l) lower limb (time 0 on the abscissa, initiation of the single stance on the right limb, r). The horizontal bars under the curves mark the single and double stance phases (black tract = right step period, grey tract = left step period). Peaks in the curvature values are labelled ssR (right single stance), dsR (right double stance), ssL (left single stance), and dsL (left double stance) along the two subsequent steps. Dashed vertical lines mark the stride phases and facilitate the comparison between different curves. Panel B zooms in on the second step (albeit encasing the last 5% of the previous step, see the abscissa), but omits the kinetic and vertical energy curves. The grey bands encase the mechanical events occurring from the ssL and dsL peaks to the return to zero curvature. It can be seen that peaks occur during a phase of zero or near-zero R (hence, of fully muscular control of walking). However, after the ssL peak, the CoM is actively braked (negative  $E_{tot}$  and power curves), whereas, after the dsL peak, the CoM is actively propelled (positive  $E_{tot}$  and power curves).

### 3.3. Curvature peaks as a potential clinical index of dynamic balance: Reproducibility

The CoM curvature patterns are shown in Fig. 3.

Curves from the twelve participants (each curve is the mean across six strides) were superimposed on a shared x-axis, giving the normalised stride period. The time course was very similar across the participants, although the peak values revealed two outliers. Besides, the changes in curvatures appeared symmetric between the left and right steps.

The curvature of the CoM path maintained the same shape across increasing walking velocities, although peaks were delayed,

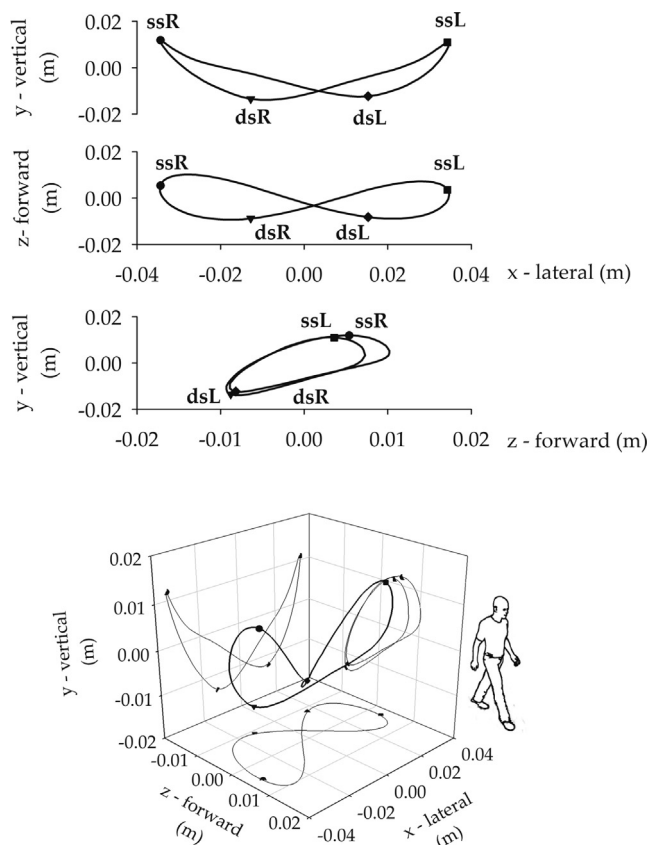
with respect to the stride normalised cycles, as the velocity increased (Fig. 4).

Fig. 5A–D gives a summary of the time delay of the curvature peaks with respect to the step initiation (onset of the single stance phase) at the different velocities tested.

Increasing velocities corresponded to smaller step durations. All four peaks were progressively anticipated (and their time of occurrence became less variable) as the step period became shorter (panels A and B), but not enough to prevent a delay in the percentage of the step duration (dsR and dsL).

The Bland-Altman plot in Fig. 6 explains the dependency of the symmetry between the right and left curvature peaks (during both





**Fig. 2.** Curvature peaks along the CoM trajectory during one stride (mean of 6 strides in a representative participant; same data as Fig. 1B). From top to bottom, the upper three curves represent the y-x, z-x, and y-z planar projections of the CoM path, respectively (coordinates given in the bottom panel). The displacement due to the mean forward velocity is subtracted. In the bottom graph, the black and grey curves refer to the 3D path of the CoM and its planar projections, respectively. Curvature peaks are labelled A-D. Peaks in the curvature values are labelled ssR (right single stance), dsR (right double stance), ssL (left single stance), and dsL (left double stance) along the two subsequent steps, as in Fig. 1, to facilitate the match among the curves shown in Figs. 1 and 2.

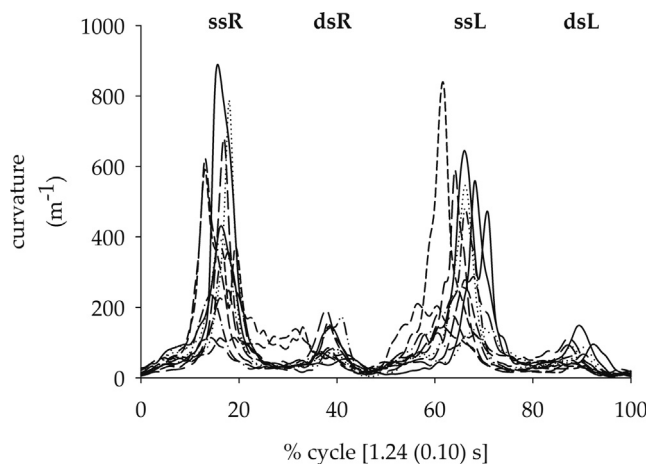


**Fig. 3.** The curvature of the CoM path ( $\text{m}^{-1}$ , on the ordinate) during one stride on a force treadmill at  $0.8 \text{ m s}^{-1}$ , as a function of the normalised stride period (on the abscissa, absolute mean duration within brackets). The stride begins with the toe-off of the right foot. Curves (mean across 6 strides) from each of the 12 participants are superimposed and are marked by distinct tracts. Peaks in the curvature values are labelled A-D along the two subsequent right and left steps. Peaks in the curvature values are labelled ssR (right single stance), dsR (right double stance), ssL (left single stance), and dsL (left double stance) along the two subsequent steps (see Fig. 1).

single and double stance) on the average amplitude of the curvature peaks.

The figure highlighted the substantial agreement between ssR and ssL (left panel, panel A), and dsR and dsL (right panel, panel B) peaks. Nineteen of the 357 steps concerning the ssR and ssL peaks (expected by chance: 18 observations, panel A), and 11 out of 296 steps concerning the dsR and dsL peaks (expected by chance: 15 observations, panel B) trespassed the tolerance limits. These results suggest a substantial right-left symmetry.

Table 2 gives numerical summaries of the information shown in Figs. 5 and 6.

The large differences between means and medians in both steps were consistent with significant non-normality in the Shapiro-Wilk tests, preventing parametric ANOVA modelling (not shown). The large differences between peaks during the single and double stance phases were significant after the Wilcoxon signed-rank test. The differences in the curvature peaks across participants and walking velocities were significant following the non-parametric Friedman ANOVA model, while the differences among ssR, dsR, ssL, and dsL were not. When contrasts between pairs of peaks were tested, no significant differences were found between ssR and ssL, while significant differences were found in all other contrasts (Supplementary Table S1).

## 4. Discussion

### a. Main findings

This study confirms that walking conceals an astonishingly refined control of the 3D curvature of the CoM, underlying its lateral oscillations. The radii of curvature were as small as 1.4–2.7 mm. Our findings are consistent with a previous paper that described for the first time the 3D trajectory of CoM during walking (Tesio et al., 2011) and highlighted the simultaneity of curvature peaks and transient annihilations of the pendulum-like mechanism during the gait cycle, implying a sudden shift from passive oscillation to a fully active, muscle-driven, control. The present study interprets the CoM path focussing on body balance, complementing the traditional “energetic” interpretations.

The energy parameters of the CoM motion are symmetric between the left and right steps (Cavagna et al., 1983; Tesio et al., 1998). The same was true at group level for CoM curvatures at all velocities tested here. However, the variability within and between participants for both curvature values and their right/left log-ratios (Table 2 and Fig. 6, respectively) was higher than that observed for energetic parameters of the CoM motion in the sagittal plane (Cavagna et al., 1983; Tesio et al., 1998). Variance was much higher for the work done to move the CoM in the frontal plane, compared to the sagittal plane (Tesio et al., 1998). One reason might be the intrinsic limits of precision of the method: measures of punctiform curvature peaks, based on angle derivatives, are inherently more noise-sensitive than energy estimates coming from double integration of forces. The sizes of the allowed periods and the required energy changes for the frontal redirection of CoM were much smaller than those characterising the CoM motion in the sagittal plane. Therefore, minor changes represent large relative variations.

### b. Fuelling the CoM motion: not only a matter of forward progression

The timing of the “external” power provided by muscles to keep the CoM in motion was already known for the sagittal plane (Cavagna et al., 1976). The main injection of muscular power takes place directly before and during the first half of the double stance (when the CoM accelerates forward more than its preceding fall

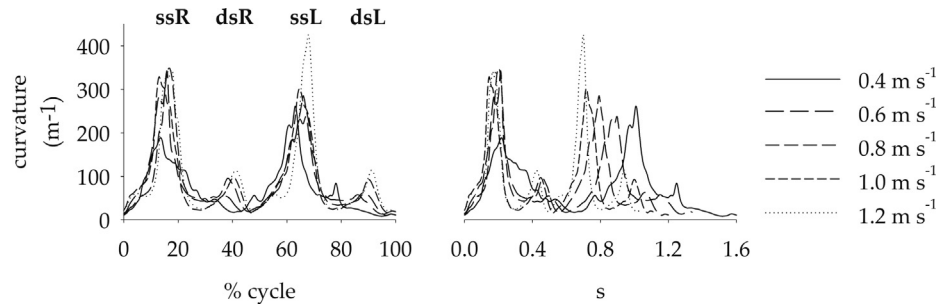


**Fig. 4.** The curvature of the CoM path during one stride (mean across 72 observations, 12 participants  $\times$  6 strides) at five different walking velocities (0.4, 0.6, 0.8, 1.0, and 1.2  $\text{m s}^{-1}$ ) as a function of the normalised stride period (on the abscissa) (left panel) and as a function of the absolute duration of the stride (right panel). Curves from the different walking velocities are marked by different tracts and superimposed. Peaks in the curvature values are labelled A-D along the two subsequent steps (see Fig. 1A for more details). Peaks in the curvature values are labelled ssR (right single stance), dsR (right double stance), ssL (left single stance), and dsL (left double stance) along the two subsequent steps (see Fig. 1A for more details).

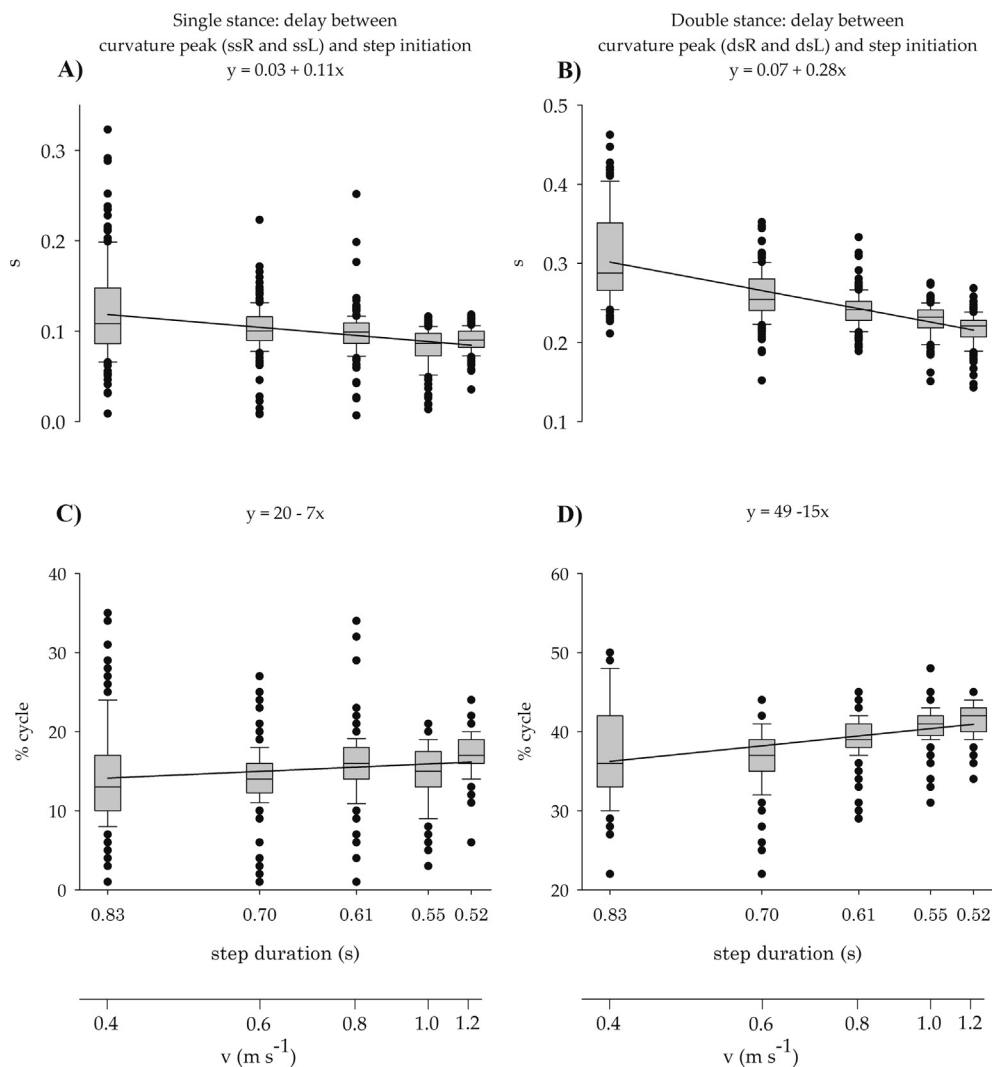


**Fig. 5.** In panels A and B (upper row) the ordinate gives the absolute time delay (s) of the peak curvature of the CoM with respect to step initiation (contralateral toe-off or the initiation of the single stance, both for left and right steps), whereas, in panels C and D (lower row), the delay is given in percentage of the step duration (the step period initiates with the single stance). The upper and lower abscissa gives the step period (s) and walking velocity ( $\text{m s}^{-1}$ ), respectively. Each box plot refers to a distinct walking velocity and summarises the results from 144 observations (12 participants  $\times$  6 steps  $\times$  2 sides) at a given velocity. The horizontal segments of the boxes encase median values and 25th–75th percentiles; whiskers extend from the 10th to the 90th percentiles; outliers are given as black circles. Note that the lower is the step duration, the higher is the velocity. Left and right panels refer to single and double stance curvature peaks (ssR or ssL, and dsR or dsL) respectively. A least square regression line is superimposed on the boxes, as a rough index of the trend.

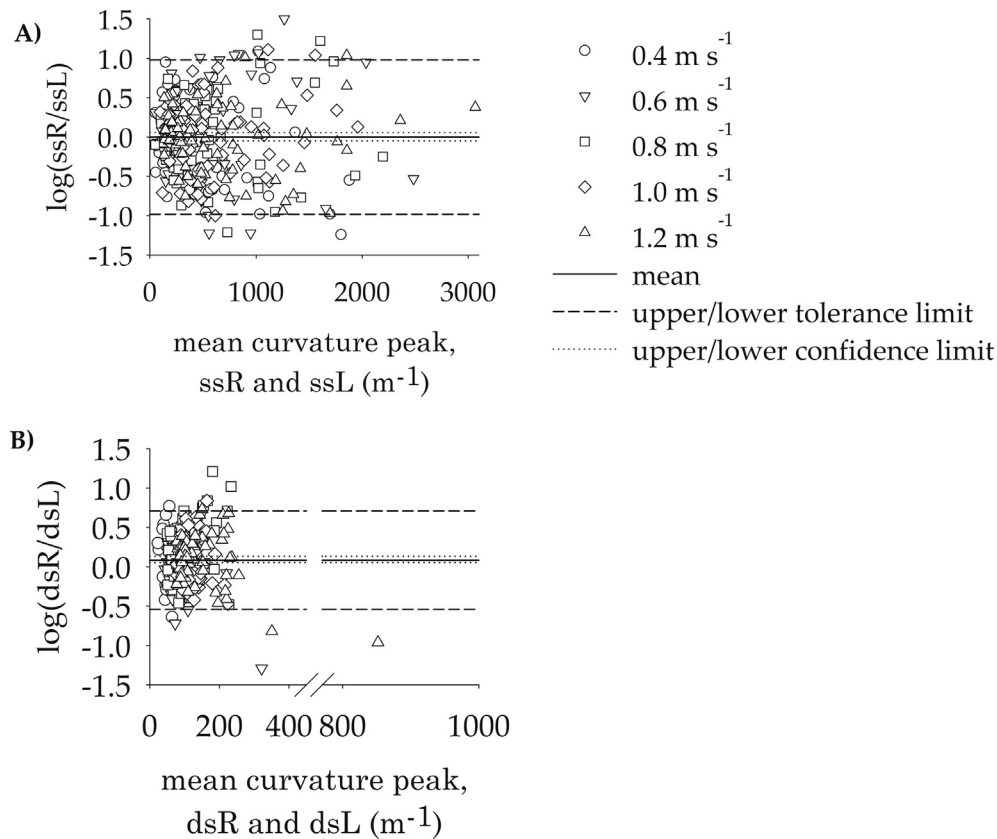


**Fig. 6.** The plots show in the left panel (panel A), the logarithm base 10 values of the ratio between the ssR and ssL curvature peak amplitudes (y-axis) versus their means (x-axis), and in the right panel (panel B), the logarithm base 10 values of the ratio between the dsR and dsL curvature peak amplitudes (y-axis) versus their means (x-axis). Solid lines report the mean of the log-ratio between the curvature peak amplitudes; dotted lines report the 95% confidence limits; dashed lines mark the 95% tolerance limits. Each symbol refers to the mean of values recorded from six subsequent strides of each study participant ( $n = 12$ ) at five walking velocities (0.4, 0.6, 0.8, 1.0, and 1.2 m s<sup>-1</sup>), represented by distinct symbols.

**Table 2**

Curvature peaks occurring during the single (ss) and double (ds) stance phases on the right (ssR and dsR) and left (ssL and dsL) steps from 12 participants (6 strides each) walking at five different velocities: 0.4, 0.6, 0.8, 1.0, and 1.2 m s<sup>-1</sup>, reported from top to bottom respectively.

Walking velocities (m s <sup>-1</sup> )	Curvature peaks (m <sup>-1</sup> ): mean (SD); medians (5th–95th percentiles)			
	Right step		Left step	
	ssR	dsR	ssL	dsL
0.4	365 (417);227 (67–1464)	132 (335);53 (14–890)	535 (671);284 (59–1895)	37 (24);30 (9–78)
0.6	548 (652);326 (65–1881)	82 (40);70 (38–143)	471 (627);242 (78–1594)	87 (78);65 (38–174)
0.8	551 (632);344 (97–1929)	125 (81);93 (49–301)	503 (605);316 (85–2117)	84 (47);80 (30–152)
1.0	593 (584);386 (112–2246)	124 (45);114 (69–215)	541 (451);380 (101–1670)	113 (50);105 (50–184)
1.2	659 (798);324 (134–2928)	150 (70);126 (75–308)	683 (684);395 (93–2221)	139 (187);96 (54–292)

SD: standard deviation.

allows), and it is mostly provided by the calf muscles of the rear limb. A 3–5 times lower injection of muscular power is required during the single stance, as a compensation for the incomplete exchange of mechanical energy (the CoM rises higher than that allowed by its former deceleration forward) (Tesio and Rota, 2019).

Motion on the frontal plane requires no more than 5% of the total external work spent during walking (Cavagna, 1975). However, as far as balance is concerned, the CoM displacement on the frontal plane is relevant. Balance impairments result in falls during walking mostly in the lateral direction (Cumming and Klineberg, 1994). Dynamic balance during walking is inherently different from static balance (Woollacott et al., 1997). Individuals may walk independently while concealing a balance deficit; this may pass undetected in routine clinical assessment.

### c. The challenge of lateral motion of the CoM

During the single stance phase, unless the walking velocity is extremely low, the lateral pendulum-like oscillation of the CoM towards the supporting side must be actively braked before the no-return point is reached, and then it must be actively braked while swinging back towards the suspended leg until the latter hits the ground. This mechanism implies a very precise dosage and sequencing between work outputs from alternating muscles. To speculate, the hip adductors of the supporting limb and contralateral paraspinal muscles might act as “brakes” of the CoM before the curvature peak is reached, while the hip abductors and the homolateral paraspinal muscles might be engaged as brakes after the peak is reached. This muscular sequence is imposed, within a

few tenths of a millisecond, on an inverted pendulum characterised by an arm of more than 1 m length, a mass of several tenths of a kilogram, and peak curvatures with radii in the order of 2–12 mm.

#### d. Neuromechanical and clinical considerations

Precise modelling of the CoM trajectory is far beyond the scope of the present article. The U-turn of the CoM is an impressive performance of neural control, though hardly detectable visually. The shorter the step period, the faster the manoeuvre must be, in an attempt to keep the U-turn event safely distant from the no-return point (see Fig. 5). During the double stance, minor curvatures are observed. In fact, there is no need for performing a U-turn on a single limb, given that the opposite leg is also on the ground and ready to be loaded. In contrast, strong positive power output is needed from the rear limb to accelerate the CoM forward and upward.

Lateral instability during walking may be due to slowed neural conduction velocity (either in the central or the peripheral nervous system): the greater the delay in conduction, the more the risk of falling (Peebles et al., 2017). Any delay in neural conduction and cortical-subcortical sensory-motor integration may affect the ability to control the mechanism subtending CoM's U-turn on time, eventually leading to falling. From this perspective, the adaptation of the amplitudes and timings of the curvature peaks to the different walking speeds might provide an index of the patient's ability to effectively control the CoM's position, in proximity of the lateral margins of stability. A more effective dynamic balance control during walking would result in earlier and higher curvature peaks in the single stance phase (i.e., narrower U-turns). Moreover, evidence from Multiple Sclerosis (Peebles et al., 2017) and Stroke (Kao et al., 2014) patients have shown greater variability in medial-lateral margins of stability in these patients during walking, when compared to healthy controls. Therefore, the widening of the base of support during walking might represent compensation for the lack of control of the U-turns of CoM.

#### e. Future scenarios

Findings of this study encourages further studies on the physiology of walking and clinical applications, such as: relationship of curvature peaks with the risk for falling and measures of static balance, their adaptation to higher walking velocities, changes in curvature peaks with age [especially during child growth (Malloggi et al., 2019a) and old age (Rogers and Mille, 2003)], relationship between curvature peaks' symmetry and asymmetric motor impairments caused by pathologies, or induced and manipulated by walking on split-belt treadmills (Tesio et al., 2021, 2017b); the extent of change in CoM curvatures during walking while bearing loads, different shoes, or orthotic devices.

In conclusion, the curvature peaks seen during single stance (ssR and ssL) provide a promising index of the capacity to maintain safe stability margins during the steps. The available xCoM and MOS indexes (see Introduction) describe the end results of joint mechanics and adaptive behaviours. In contrast, the curvature peaks shed light on the underlying neural control of the lateral oscillations of CoM. Correspondingly, they provide a stimulus for deeper biomechanical and neurophysiological studies and represent a balance index that complements the existing ones.

#### Declaration of Competing Interest

The authors declare that they have no known competing financial interests or personal relationships that could have appeared to influence the work reported in this paper.

#### Appendix A. Supplementary data

Supplementary data to this article can be found online at <https://doi.org/10.1016/j.jbiomech.2021.110486>.

#### References

- Alexander, R.M., 2005. Physiology. Walking made simple. *Science* 308 (80), 58–59. <https://doi.org/10.1126/science.1111110>.
- Altman, D.G., Bland, J.M., 1983. Measurement in medicine: the analysis of method comparison studies. *Stat.* 32, 307–311.
- Bauby, C.E., Kuo, A.D., 2000. Active control of lateral balance in human walking. *J. Biomech.* 33, 1433–1440. [https://doi.org/10.1016/S0021-9290\(00\)00101-9](https://doi.org/10.1016/S0021-9290(00)00101-9).
- Bierbaum, S., Peper, A., Karamanidis, K., Arampatzis, A., 2010. Adaptational responses in dynamic stability during disturbed walking in the elderly. *J. Biomech.* 43, 2362–2368. <https://doi.org/10.1016/j.jbiomech.2010.04.025>.
- Cavagna, G.A., 1975. Force platforms as ergometers. *J. Appl. Physiol.* 39, 174–179. <https://doi.org/10.1152/jappl.1975.39.1.174>.
- Cavagna, G.A., Thys, H., Zamboni, A., 1976. The sources of external work in level walking and running. *J. Physiol.* 262, 639–657.
- Cavagna, G.A., Tesio, L., Fuchimoto, T., Heglund, N.C., 1983. Ergometric evaluation of pathological gait. *J. Appl. Physiol.* 55, 607–613. <https://doi.org/10.1152/jappl.1983.55.2.606>.
- Cavagna, G.A., Willems, P.A., Legramandi, M.A., Heglund, N.C., 2002. Pendular energy transduction within the step in human walking. *J. Exp. Biol.* 205, 3413–3422.
- Cumming, R., Klineberg, R., 1994. Fall frequency and characteristics and the risk of hip fractures. *J. Am. Geriatr. Soc.* 42, 774–778.
- Gates, D.H., Scott, S.J., Wilken, J.M., Dingwell, J.B., 2013. Frontal plane dynamic margins of stability in individuals with and without transtibial amputation walking on a loose rock surface. *Gait Posture* 38, 570–575. <https://doi.org/10.1016/j.gaitpost.2013.01.024>.
- Hak, L., Houdijk, H., van der Wurff, P., Prins, M.R., Mert, A., Beek, P.J., van Dieën, J.H., 2013. Stepping strategies used by post-stroke individuals to maintain margins of stability during walking. *Clin. Biomech.* 28, 1041–1048. <https://doi.org/10.1016/j.clinbiomech.2013.10.010>.
- Hof, A.L., 2007. The equations of motion for a standing human reveal three mechanisms for balance. *J. Biomech.* 40, 451–457. <https://doi.org/10.1016/j.jbiomech.2005.12.016>.
- Hof, A.L., 2008. The 'extrapolated center of mass' concept suggests a simple control of balance in walking. *Hum. Mov. Sci.* 27, 112–125. <https://doi.org/10.1016/j.humov.2007.08.003>.
- Hof, A.L., Gazendam, M.G.J., Sinke, W.E., 2005. The condition for dynamic stability. *J. Biomech.* 38, 1–8. <https://doi.org/10.1016/j.jbiomech.2004.03.025>.
- Hof, A.L., van Bockel, R.M., Schoppen, T., Postema, K., 2007. Control of lateral balance in walking: experimental findings in normal subjects and above-knee amputees. *Gait Posture* 25, 250–258. <https://doi.org/10.1016/j.gaitpost.2006.04.013>.
- Hurt, C.P., Grabiner, M.D., 2015. Age-related differences in the maintenance of frontal plane dynamic stability while stepping to targets. *J. Biomech.* 48, 592–597. <https://doi.org/10.1016/j.jbiomech.2015.01.003>.
- Hurt, C.P., Rosenblatt, N.J., Grabiner, M.D., 2011. Form of the compensatory stepping response to repeated laterally directed postural disturbances. *Exp. Brain Res.* 214, 557–566. <https://doi.org/10.1007/s00221-011-2854-1>.
- Kao, P.-C., Dingwell, J.B., Higginson, J.S., Binder-MacLeod, S., 2014. Dynamic instability during post-stroke hemiparetic walking. *Gait Posture* 40, 457–463. <https://doi.org/10.1016/j.gaitpost.2014.05.014>.
- MacKinnon, C.D., Winter, D.A., 1993. Control of whole body balance in the frontal plane during human walking. *J. Biomech.* 26, 633–644. [https://doi.org/10.1016/0021-9290\(93\)90027-C](https://doi.org/10.1016/0021-9290(93)90027-C).
- Malloggi, C., Catino, L., Rota, V., Perucca, L., Scarano, S., Tesio, L., 2019a. The path curvature of the body centre of mass during walking as an index of balance control in patients with Multiple Sclerosis. *World Congress. International Society of Posture and Gait Research (ISPGR)*.
- Malloggi, C., Rota, V., Catino, L., Malfitano, C., Scarano, S., Soranna, D., Zamboni, A., Tesio, L., 2019b. Three-dimensional path of the body centre of mass during walking in children: an index of neural maturation. *Int. J. Rehabil. Res.* 42, 112–119. <https://doi.org/10.1097/MRR.0000000000000345>.
- Mc Andrew Young, P.M., Wilken, J.M., Dingwell, J.B., 2012. Dynamic margins of stability during human walking in destabilizing environments. *J. Biomech.* 45, 1053–1059. <https://doi.org/10.1016/j.jbiomech.2011.12.027>.
- Okubo, Y., Brodie, M., Sturmeiks, D., Hicks, C., Carter, H., Toson, B., Lord, S.R., 2018. Exposure to unpredictable trips and slips while walking can improve balance recovery responses with minimum predictive gait alterations. *PLoS ONE* 13. <https://doi.org/10.1371/journal.pone.0202913>.
- Peebles, A.T., Brutsch, A.P., Lynch, S.G., Huisinga, J.M., 2017. Dynamic balance in persons with multiple sclerosis who have a falls history is altered compared to non-fallers and to healthy controls. *J. Biomech.* 63, 158–163. <https://doi.org/10.1016/j.jbiomech.2017.08.023>.
- Rogers, M., Hedman, L., Johnson, M., Cain, T., Hanke, T., 2001. Lateral stability during forward-induced stepping for dynamic balance recovery in young and older adults. *J. Gerontol. A Biol. Sci. Med. Sci.* 56A, M589–M594. <https://doi.org/10.1093/gerona/56.9.m589>.



- Rogers, M.W., Mille, M.-L., 2003. Lateral stability and falls in older people. *Exerc. Sport Sci. Rev.* 31, 182–187. <https://doi.org/10.1097/00003677-200310000-00005>.
- Rosenblatt, N.J., Grabiner, M.D., 2010. Measures of frontal plane stability during treadmill and overground walking. *Gait Posture* 31, 380–384. <https://doi.org/10.1016/j.gaitpost.2010.01.002>.
- Rota, V., Benedetti, M.G., Okita, Y., Manfrini, M., Tesio, L., 2016. Knee rotationplasty: motion of the body centre of mass during walking. *Int. J. Rehabil. Res.* 39, 346–353. <https://doi.org/10.1097/MRR.0000000000000195>.
- Siragy, T., Nantel, J., 2018. Quantifying dynamic balance in young, elderly and Parkinson's individuals: a systematic review. *Front. Aging Neurosci.* 10, 387. <https://doi.org/10.3389/fnagi.2018.00387>.
- Smeesters, C., Hayes, W.C., McMahon, T.A., 2001. Disturbance type and gait speed affect fall direction and impact location. *J. Biomech.* 34, 309–317. [https://doi.org/10.1016/S0021-9290\(00\)00200-1](https://doi.org/10.1016/S0021-9290(00)00200-1).
- Tesio, L., Scarano, S., Cerina, V., Malloggi, C., Catino, L., 2021. Velocity of the body center of mass during walking on split-belt treadmill. *Am. J. Phys. Med. Rehabil.* Volume Publish Ahead of Print. <https://doi.org/10.1097/PHM.0000000000001674>.
- Tesio, L., Lanzi, D., Detrembleur, C., 1998. The 3-D motion of the centre of gravity of the human body during level walking. I. Normal subjects at low and intermediate walking speeds. *Clin. Biomech.* 13, 77–82. [https://doi.org/10.1016/S0268-0033\(97\)00080-6](https://doi.org/10.1016/S0268-0033(97)00080-6).
- Tesio, L., Rota, V., 2008. Gait analysis on split-belt force treadmills: validation of an instrument. *Am. J. Phys. Med. Rehabil.* 87, 515–526. <https://doi.org/10.1097/PHM.0b013e31816f17e1>.
- Tesio, L., Rota, V., Chessa, C., Perucca, L., 2010. The 3D path of body centre of mass during adult human walking on force treadmill. *J. Biomech.* 43, 938–944. <https://doi.org/10.1016/j.jbiomech.2009.10.049>.
- Tesio, L., Rota, V., 2019. The motion of the body center of mass during walking: a review oriented to clinical applications. *Front. Neurol.* 10. <https://doi.org/10.3389/fneur.2019.00999>.
- Tesio, L., Rota, V., Perucca, L., 2011. The 3D trajectory of the body centre of mass during adult human walking: Evidence for a speed-curvature power law. *J. Biomech.* 44, 732–740. <https://doi.org/10.1016/j.jbiomech.2010.10.035>.
- Tesio, L., Rota, V., Malloggi, C., Brugliera, L., Catino, L., 2017b. Crouch gait can be an effective form of forced-use/no constraint exercise for the paretic lower limb in stroke. *Int. J. Rehabil. Res.* 40, 254–267. <https://doi.org/10.1097/MRR.0000000000000236>.
- Vistamehr, A., Kautz, S.A., Bowden, M.G., Neptune, R.R., 2016. Correlations between measures of dynamic balance in individuals with post-stroke hemiparesis. *J. Biomech.* 49, 396–400. <https://doi.org/10.1016/j.jbiomech.2015.12.047>.
- Woollacott MH, T.P.F., 1997. Balance control during walking in the older adult: research and its implications. *Phys. Ther.* 77, 646–660.